Matrix metalloproteinase-2 governs lymphatic vessel formation as an interstitial collagenase

*Benoit Detry,[1] *Charlotte Erpicum,[1] *Jenny Paupert,[1] Silvia Blacher,[1] Catherine Maillard,[1] Françoise Bruyère,[2] Hélène Pendeville,[3] Thibault Remacle,[1] Vincent Lambert,[1-4] Cédric Balsat,[1] Sandra Ormenese,[5] Françoise Lamaye,[6] Els Janssens,[7] Lieve Moons,[7] Didier Cataldo,[1] Frédéric Kridelka,[8] Peter Carmeliet,[2] Marc Thiry,[6] Jean-Michel Foidart,[1] Ingrid Struman,[3] and Agnès Noel[1]

[1]Laboratory of Tumor and Development Biology, Groupe Interdisciplinaire de Génoprotéomique Appliqué-Recherche (GIGA-Cancer), University of Liège, Liège, Belgium; [2]Laboratory of Angiogenesis and Neurovascular Link, Vesalius Research Center, Vlaams Instituut voor Biotechnologie–KULeuven, Leuven, Belgium; [3]Unit of Molecular Biology and Genetic Engineering, GIGA-Cancer, University of Liège, Liège, Belgium; [4]Department of Ophthalmology, Centre Hospitalier Universitaire (CHU) Liège, Liège, Belgium; [5]GIGA-Imaging and Flow Cytometry Platform, and [6]Laboratory of Cell and Tissue Biology, GIGA-Neurosciences, University of Liège, Liège, Belgium; [7]Laboratory of Neural Circuit Development and Regeneration, Biology Department, KULeuven, Leuven, Belgium; and [8]Department of Obstetrics and Gynecology, CHU Liège, Liège, Belgium

Lymphatic dysfunctions are associated with several human diseases, including lymphedema and metastatic spread of cancer. Although it is well recognized that lymphatic capillaries attach directly to interstitial matrix mainly composed of fibrillar type I collagen, the interactions occurring between lymphatics and their surrounding matrix have been overlooked. In this study, we demonstrate how matrix metalloproteinase (MMP)–2 drives lymphatic morphogenesis through *Mmp2*-gene ablation in mice, *mmp2* knockdown in zebrafish and in 3D-culture systems, and through MMP2 inhibition. In all models used in vivo (3 murine models and thoracic duct development in zebrafish) and in vitro (lymphatic ring and spheroid assays), MMP2 blockage or down-regulation leads to reduced lymphangiogenesis or altered vessel branching. Our data show that lymphatic endothelial cell (LEC) migration through collagen fibers is affected by physical matrix constraints (matrix composition, density, and cross-linking). Transmission electron microscopy and confocal reflection microscopy using DQ-collagen highlight the contribution of MMP2 to mesenchymal-like migration of LECs associated with collagen fiber remodeling. Our findings provide new mechanistic insight into how LECs negotiate an interstitial type I collagen barrier and reveal an unexpected MMP2-driven collagenolytic pathway for lymphatic vessel formation and morphogenesis. (*Blood*. 2012;119(21):5048-5056)

Introduction

Lymphatic vessels are essential for body fluid balance and immunologic surveillance. Several pathologies manifest abnormal lymphatic vessel growth (lymphangiogenesis), either excessive (inflammatory diseases, tumor metastases, cornea-graft rejection) or defective (lymphedema).[1-3] Our understanding of the molecular mechanisms underlying lymphangiogenesis is still in its infancy. Although several key molecular determinants (vascular endothelial growth factor [VEGF]-C/D, VEGF receptor-3, angiopoietin, ephrins, integrins, etc) have been identified,[2,4-7] the importance of cell-matrix interactions during the lymphangiogenic process is not well documented.

One of the features that discriminates lymphatic capillaries from blood capillaries is the kind of extracellular matrix (ECM) to which each vessel type is exposed in its natural environment. Blood vascular endothelium is in direct contact with basement membrane components (laminin, type IV collagen),[8] whereas the basal lamina is largely absent in lymphatic capillaries. Lymphatic endothelial cells (LECs) interact intimately with the adjacent interstitial matrix and attach to it through anchorage filaments.[9,10] Therefore, LECs sprouting from preexisting vessels and their migration through the ECM require that they be able to negotiate an interstitial collagen barrier mainly composed of fibrillar type I collagen. Recently, evidence has accumulated demonstrating that integrins, by promoting cell-matrix interaction, influence normal lymphatic function and lymphangiogenesis.[5,10,11] How LECs deal with fibrillar collagens to migrate and form new lymphatics has not yet been documented. Migration across the ECM is mainly protease-dependent,[12] although it has been reported that some cells, such as cancer cells, could squeeze through fibrillar collagen by adopting an ameboid phenotype in a protease-independent way.[13]

Matrix metalloproteinases (MMPs) are key regulators of matrix remodeling.[14] Although their important role in angiogenesis is now established, their contribution during lymphangiogenesis has received limited attention. Among MMPs, MMP2, and MMP9 are produced by LECs[15,16] and synthetic MMP inhibitors inhibited LEC tube formation.[16] MMP2 function has long been limited to basement membrane degradation through its capacity to cleave type IV collagen. In this context, our previous discovery that MMP2 but not MMP9 deficiency impaired in vitro LECs sprouting from the thoracic duct (TD)[15] was unexpected and highlighted a

Submitted December 21, 2011; accepted March 25, 2012. Prepublished online as *Blood* First Edition paper, April 6, 2012; DOI 10.1182/blood-2011-12-400267.

*B.D., C.E., and J.P. contributed equally to this work.

The online version of this article contains a data supplement.

The publication costs of this article were defrayed in part by page charge payment. Therefore, and solely to indicate this fact, this article is hereby marked "advertisement" in accordance with 18 USC section 1734.

key MMP role in lymphangiogenesis, rather than the initially described minor role.[10] However, how MMP2 regulates lymphangiogenesis remains an intriguing enigma. In addition to ECM components, numerous substrates were identified (primarily in vitro) for MMP2, such as growth factors (TGFβ, FGF receptor-1, pro-TNF, IL-1β), chemokines, and angiogenic inhibitors (connective tissue growth factor,[17] pleiotrophin; for review, see Bauvois,[18] Cauwe[19] and Kessenbrock[14]).

In this study, we explored MMP2 mechanisms of action in lymphangiogenesis using different in vitro and in vivo models. We provide evidence that MMP2 contributes to the elaboration of lymphatic vessels under physiologic and pathologic conditions, by acting as an interstitial collagenase, easing cell passage through physical barriers and controlling vessel branching. These findings plead for a reevaluation of the MMP2 contribution to interstitial tissue remodeling and highlight MMP2 participation in lymphangiogenesis.

Methods

Zebrafish

Transgenic Fli1:eGFP^{y} and Stab1:YFP zebrafish (*Danio rerio*) lines were maintained in the GIGA-Zebrafish Facility (University of Liège, Belgium). Stab1:YFP transgenic line was provided by Pr. Schulte-Merker (Hubrecht Institute, Utrecht, The Netherlands) and Fli1:eGFP^{y} were from ZIRC (Oregon University). One-cell stage embryos were injected with morpholino oligonucleotides (*MO*; 0.5 ng/embryo) targeting *mmp2* (*MOmmp2*; 5′-GGGAGCTTAGTAAACACAAACCTGT-3′), or a standard control *MO* (*MOctl*) designed by Gene Tools. *MOctl* or *MOmmp2* was injected into transgenic Fli1:eGFP^{y} zebrafish (n = 169 and n = 149) or Stab1:YFP zebrafish (n = 124 and n = 143) in the presence of 0.5% Rhodamine dextran to check injection efficiency. To visualize the TD, embryos were anesthetized with tricaine (Sigma-Aldrich), mounted in 3% methyl cellulose and observed under an Eclipse 90*i* fluorescence microscope (Nikon).

For whole-mount in situ hybridization carried out according to Thisse et al,[20] embryos were fixed overnight in 4% paraformaldehyde and stored in 100% methanol at −20°C. Antisense digoxigenin-labeled RNA probes were synthesized according to the manufacturer's instructions (Roche Applied Science). The following primers were used for polymerase chain reaction (PCR)–amplification: sense: 5′-TTCTTGCTTCCCTGCAAACT-3′ and antisense: 5′-GCTCCTGGATGCCTTTAACA-3′. For sectioning, embryos were embedded in a mixture of 0.5% gelatin, 30% BSA, and 20% sucrose dissolved in PBS. Polymerization was achieved using 25% glutaraldehyde. Sections were made on a Campden Instruments vibratome and visualized under a BX60 microscope (Olympus).

Transgenic mice

Homozygous *Mmp2*-deficient mice (*Mmp2* KO) and their corresponding wild-type (WT) strain of either sex were used throughout the study.[21] More than 10 backcrosses to C57BL/6 background were done before analysis. Animal experiments were performed in compliance with the Animal Ethics Committee of the University of Liège.

Corneal lymphangiogenesis assay

Corneal lymphangiogenesis was induced by thermal cauterization with an ophthalmic cautery (Optemp II V; Alcon Surgical) as previously described.[22] Seven or 14 days later, mice were killed and the eyes were removed and dissected. Whole-mounted corneas (n = 10) were immunostained with polyclonal goat anti–mouse lymphatic vessel endothelial receptor-1 (LYVE-1; 1/200; R&D Systems) and Alexa Fluor 488–coupled rabbit anti–goat antibody (1/200; Molecular Probes). A previously described computerized method[23] was used to quantify the lymphangiogenic response by determining the area covered by lymphatics (vessel), the number of vessels (end point), the number of bifurcations (branching), and the total vessel length (length). All results normalized to the total cornea area were expressed as densities.

For reverse transcription (RT)–PCR analysis, frozen tissues were pulverized (MagNA Lyser; Roche) and total RNA was extracted with a kit (RNeasy; QIAGEN), according to the manufacturer's protocol. Mmp2 mRNA and 28S rRNA were amplified with a 10-ng aliquot of total RNA using an amplification kit (GeneAmp Thermostable rTth Reverse Transcriptase RNA PCR Kit; Roche) and the following primers (Eurogentec): sense: 5′-GTTCACCCACTAATAGGGAACGTGA-3′ and antisense: 5′-GGATTCTGACTTAGAGGCCTTCAGT-3′ for 28S; sense: 5′-GCTGGTCAGTGGCTTGGGGTA-3′ and antisense: 5′-AGATCTTCTTCTTCAAGGACCGGTT-3′ for Mmp2. Reverse transcription was performed at 70°C for 15 minutes followed by RNA–DNA heteroduplex denaturation at 94°C. Amplification (18 cycles for 28S and 30 cycles for Mmp2) started by a 15-second cycle at 94°C, 20 seconds at 68°C, and 10 seconds at 72°C. RT-PCR products were resolved in 10% acrylamide gels after staining with Gel Star (Cambrex). The expected sizes of RT-PCR products were 212 bp for 28S and 225 bp for Mmp2.

Tail and ear whole-mount preparations

Mice (n = 5) were killed and tail or ear dermal sheets were prepared as previously described[24] before immunolabeling conducted as described for corneas, and whole-mounted. For ear lymphatic vessels, computerized image-analysis method was used to determine 4 different parameters: vessel, length, end point, and branching densities.[23] For tail, image processing of lymphatic vasculature included: noise elimination by low pass filter in original stacked images and image binarization using automatic threshold (Matlab 7.9; The Mathworks). For each binary image, skeleton was determined and branching points as well as lymphatic rings were identified. The following measurements were performed: the length of skeleton by unit of vessel area, the number of branchings by unity of vessel area, and the mean area of rings. For both tail and ear preparations, at least 5 images were quantified per condition (n = 5 mice) and all parameters were normalized to the total sample area (densities).

Lymphatic ring assay

3-D lymphatic ring cultures were performed as previously described.[15] Briefly, TD dissected from mice (2-4 months old) were cut into 1-mm pieces. In standard assays, the explants were embedded in interstitial type I collagen gel (pepsinized collagen; 1.5 mg/mL) and cultured for 7 to 11 days, in MCDB131 (Invitrogen) supplemented with 4% Ultroser G (BioSepra). When indicated, lymphatic rings were embedded in native collagen. In some assays, increasing doses of rmMMP2 (R&D Systems) were added to culture medium. To avoid MMP2 interference from Ultroser, MMP2 depletion was achieved through Ultroser incubations with gelatin–Sepharose-4B (GE Healthcare). Computerized quantifications were performed on binary images as previously described.[15] A grid of concentric rings was generated by successive increments at fixed intervals of TD boundary. Then, the number of microvessel-grid intersections was counted and plotted versus the distance from the ring to determine microvessel distribution. At least 5 images per experimental condition were used. To determine significant differences between experimental conditions, values obtained at 0.25 mm, 0.5 mm, or 0.75 mm from the ring were compared with Student *t* test.

LEC culture, collagen-gel preparation, and spheroid assay

Human telomerase-transfected dermal LECs (HTERT-HDLECs)[25] were grown in EGM2-MV medium (Lonza; Invitrogen) supplemented with 5% FCS and L-glutamine (Invitrogen). VEGFR3 expression was checked by RT-PCR. Tissue inhibitor of metalloproteinase-2 (TIMP2) was purified from Chinese hamster ovary cells expressing TIMP2.[26] Specific MMP2 inhibitor was purchased from Calbiochem and siRNA from ThermoScientific. LEC were transfected with siRNA through calcium–phosphate precipitation and *MMP2* knockdown efficiency was determined by RT-PCR. For LEC cultures in 3D collagen matrix, 2 collagen preparations

were used: pepsin-extracted type I collagen (pepsinized collagen; Collagen R, Serva Electrophoresis), and telopeptide-intact collagen (native collagen) extracted from rat tail tendons.[27]

To generate multicellular spheroids, HTERT-HDLECs cells[25] were seeded in endothelial basal medium (EBM)–2 medium containing 0.24% high viscosity methyl cellulose (Sigma-Aldrich; 2×10^3 cells per well).[28] After 24 hours of culture, the spheroids were collected, embedded in collagen gels and maintained at 37°C, for 24 hours, in 5% FCS supplemented medium for standard cultures or MMP2-depleted serum for siRNA transfection. Computer-assisted quantification adapted from the lymphatic ring assay[15] was used to determine cell migration, which is expressed as cell density plotted versus the distance from spheroid.

For time-lapse imaging, spheroids were incorporated into dequenched (DQ) FITC collagen (Invitrogen) lattices (1 μL/200 μL of native collagen). Serial time-lapse images were acquired at 3-minute intervals with an inverted confocal laser-scanning microscope (Olympus FV1000) using 488- and 561-nm lasers. Cell morphology was monitored by transmission using the 561-nm laser and collagen cleavage by FITC fluorescence after excitation at 488 nm. Intracellular collagen fragments were detected by cell membrane labeling with PKH26 red fluorescent cell linker (Sigma-Aldrich). For the visualization of collagen-fiber remodeling by reflection, samples were illuminated with a 488-nm laser and the reflected light was detected in a photomultiplier 1 (with a spectral detector window at 470-503 nm) after being reflected by a 510-nm short-pass filter.

Lymphangioma

Lymphangioma or lymphatic endothelial hyperplasia was induced by 2 intraperitoneal injections of incomplete Freund adjuvant with a 15-day interval.[29,30] For ethical reasons, buprenorphine (0.05 mg/kg) was injected 1 hour before and after adjuvant injections, and every 12 hour during the first 5 days after injection. After 4 weeks, the diaphragms were harvested and used for transmission electron microscopy (TEM).

TEM

Samples were washed in Sörensen buffer, fixed with 2.5% glutaraldehyde in a 0.1-mol/L Sörensen phosphate buffer (pH 7.4), and postfixed with 1% osmium tetroxide.[22] Ultrathin sections of samples embedded in Epon were contrast-stained with uranyl acetate and lead citrate.[22] Observations were made with a Jeol 100 CX II TEM at 60 kV.

Results

Mmp2 deficiency affects lymphatic vessel development under physiologic conditions

To explore the impact of *Mmp2* ablation on the establishment of normal lymphatic vasculature in mice, we first examined the tail dermal lymphatic network that forms during the first postnatal week. Mature superficial dermal lymphatic vessels have a honeycomb profile, consisting of a hexagonal lattice of capillaries containing the so-called lymphatic ring complex (LRC) at each junction.[31] On postnatal day 1 or 2, only a few single-ringed LRCs were observed. During lymphatic development, LRC complexity increases through a sprouting process, leading to the formation of multiringed structures finally containing 4 to 6 rings. Original computer-assisted methods were set up to analyze LRC complexity in whole-mounted tail skin of *Mmp2*-deficient and WT mice (on postnatal days 5 and 11; Figure 1A-B). On day 5, *Mmp2*-gene knockout (KO) significantly affected ring development, leading to increased ring area (Figure 1C). The computerized evaluation of vessel skeleton (Figure 1D) revealed increased vessel density and vessel branchings (Figure 1E). Altogether these data highlight a more branched and complex network of lymphatic vessels in the absence of *Mmp2* during development. At day 11, all parameters measured were similar in both genotypes suggesting a transient impact of *Mmp2* gene ablation on lymphatic vasculature (Figure 1C-E). When we examined lymphatic vasculature in the ear of adult mice, no differences in terms of vasculature density and branchings were observed between the 2 genotypes (data not shown).

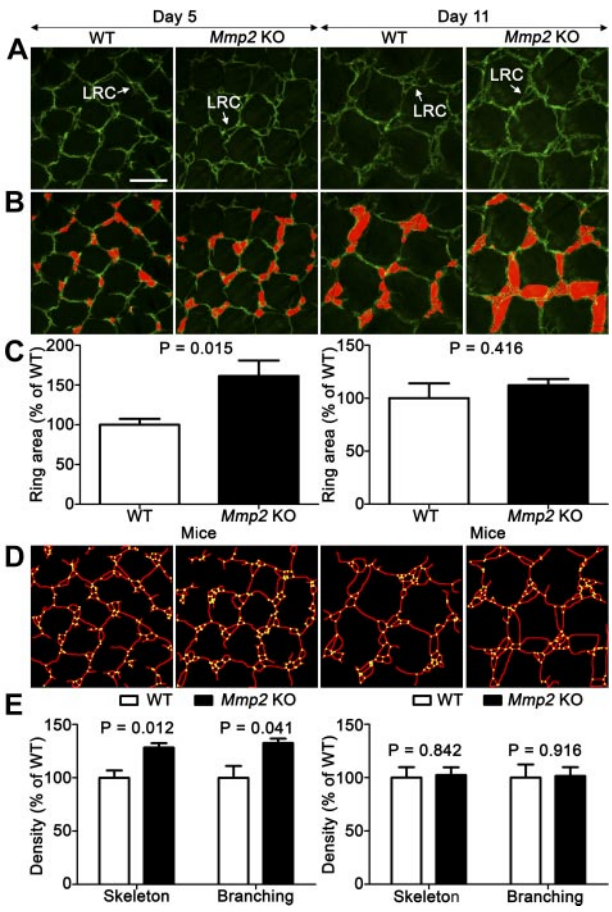

Figure 1. *Mmp2* deficiency affects early tail dermal lymphangiogenesis. (A) Dermal lymphatic vasculature is visualized in *Mmp2*-deficient mice (*Mmp2* KO) and WT mice by whole-mount LYVE-1 immunohistochemistry on postnatal days 5 and 11. LRC forming in the honeycomb network is delineated on original pictures (white arrow; A) and outlined in red through a computerized method (B). Images in panels A and B are representative of at least 40 images (n = 5). (C) Mean ring-area was determined with a computerized method as described in "Tail and ear whole-mount preparations." The densities of vessel skeleton (delineated in red) and intersections (yellow points; D) were determined by a computer-assisted method (E). Results are expressed as percentage of control. Error bars indicate SEM. Bars represent 200 μm in each panel. Tissues stained with Alexa Fluor 488 (Molecular Probes) were used mounted in Vectashield mounting medium (Vector Laboratories) and excited using a multi-Argon laser. Panels are Z-stack average projections of Z-series pictures that were acquired at room temperature, on a TCS SP2 confocal microscope (Leica Microsystems) with a 2 μm step size using Leica Confocal 2.5 acquisition software (Leica) and a 10× NA 0.3 HC PL FLUOTAR lens (Leica).

The zebrafish was next used as a developmental system (Figure 2). The zebrafish *mmp2* homologue shares > 80% identity with its human counterpart (*MMP2*) and is expressed as early as the 1-cell stage.[32] Its expression in areas of blood and lymphatic vessel formation was checked by in situ hybridization (Figure 2A). In zebrafish, the TD is located between the dorsal aorta and the posterior cardinal vein. Its development starts around 30 to 50 hours after fertilization and is finalized at 3 to 6 days postfertilization (dpf).[33] *Mmp2* expression was knocked down by injecting morpholinos (*MOmmp2*) into 1-cell stage Fli1:eGFP^y embryos (morphant embryos). Different morpholino concentrations were tested to determine submaximal doses that did not affect morphant

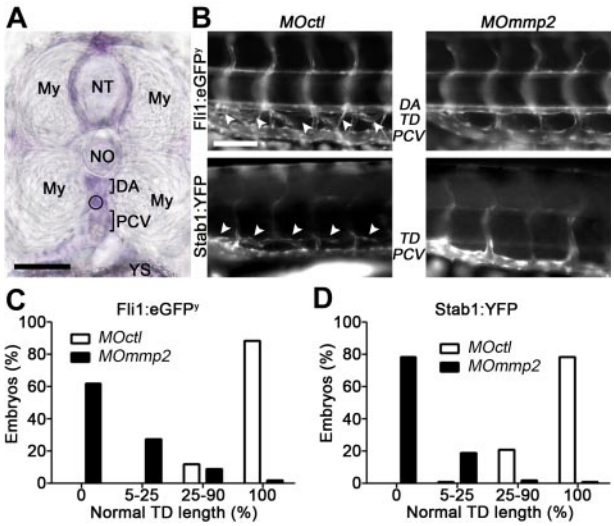

Figure 2. *Mmp2* knockdown impairs TD formation in zebrafish. (A) *Mmp2* mRNA expression (purple staining) analyzed by whole-mount in situ hybrization in 3 days postfertilization (dpf) zebrafish embryos. *Mmp2* mRNA expression is visualized between the 2 myotomes (My), around the neural tube (NT), and below the notochord (NO) where the TD is under formation (circle), in the space between the dorsal aorta (DA) and the posterior-cardinal vein (PCV). YS indicates yolk sac. (B) One-cell transgenic Fli1:eGFP^{y} and Stab1:YFP zebrafish embryos were injected with control (*MOctl*) or anti-*mmp2* (*MOmmp2*) morpholino oligonucleotides. In 5 dpf control Fli1:eGFP^{y} (top left picture), the TD (white arrow heads) is visible between the DA and the PCV. In control Stab1:YFP zebrafish (bottom left picture), the TD (white arrow heads) is seen above the PCV. Morphant embryos have TD defects (right). (C-D) Quantification of the defective TD formation at 5 dpf. The percentages of embryos with severe (no vessel, 0), drastic (5%-25% of normal TD length), moderate (25%-90% normal TD length), and no (100% normal TD length) lymphatic defects were determined for both transgenic lines after injection of control or anti-*mmp2* (*MOmmp2*) morpholinos. Bars represent 50 μm (A) and 100 μm (B). In panel A, tissue was used mounted in 3% methyl cellulose and images were captured at room temperature with BX60 microscope (Olympus) coupled to DP70 digital camera (Olympus), using acquisition software CellA 3.3 (Olympus Soft Imaging Solutions) and a 40× NA 0.75 VPlan FI lens (Olympus). In panel B, green fluorescent protein or yellow fluorescent protein expressing tissues were used mounted in 3% methyl cellulose and observed immediately under an Eclipse 90*i* fluorescent microscope (Nikon Instruments). Images were captured at room temperature, with DXM1200C Digital Camera (Nikon Instruments), with acquisition software NIS-Elements 3.00 (Nikon Laboratory Imaging) and a 20× NA 0.5 DIC M/N2 lens (Nikon). Pictures were converted to black and white using Photoshop CS4 software (Adobe Systems).

embryo morphology (ie, normal body size, trunk circulation, without retarded development, tissue malformation, or toxic sign). RT-PCR analysis demonstrated that the chosen dose (0.5 ng) affected mmp2 mRNA expression but not embryo morphology. After control morpholino (*MOctl*) injection, the TD developed as a continuous vessel by 5 dpf (Figure 2B). In contrast, *MOmmp2* injection caused dramatic lymphangiogenesis defects (Figure 2B). The percentages of embryos with severe (no vessel, lymphatic abrogation), drastic (5%-25% of normal TD length), moderate (25%-90% normal TD length), or no (100% normal TD length) lymphatic vessel defects were determined. At 5 dpf, the TD failed to form in 62% of morphant embryos and exceeded its normal length by 5%-25% in 28% of 149 embryos (Figure 2C). In sharp contrast, > 90% of 169 embryos injected with a control *MOctl* had normal length TD (Figure 2C). To easily observe embryonic lymphangiogenesis, we took advantage of Stab1:YFP zebrafish expressing the reporter gene only in venous endothelial cells and LECs. Similar results were obtained with Stab1:YFP zebrafish, with 79% of 143 morphants completely lacking a TD by 5 dpf (Figure 2D). At 7 dpf, morphants suffered severe edema and all of them died by 9 dpf, reflecting an irreversible phenotype and the absence of compensatory mechanisms to reverse the lymphatic defect induced by *mmp2* knockdown. At 0.5-ng MO dose used, no major blood vessel defect was seen in morphants, demonstrating that the lymphatic defect did not result from defective angiogenesis.

Mmp2 deficiency in mice affects pathologic lymphangiogenesis

In a corneal lymphangiogenesis model induced by thermal cauterization, RT-PCR analysis revealed baseline Mmp2 mRNA expression under physiologic conditions (day 0) and up-regulated expression at day 7 ($P < .05$) and 14 after cauterization ($P < .001$; Figure 3A). The day 7 lymphatic vascular structure was evaluated on flat mounted corneas after immunolabeling with an anti–LYVE-1 antibody (Figure 3B). It was first globally analyzed using a computerized method, by determining vessel distribution at a distance from the corneal limbus from which they emerged (Figure 3C), and by measuring total vessel-area density (Figure 3D) and total vessel-length density (Figure 3E). Vessel growth was significantly more abundant in the absence of *Mmp2*. To assess vascular network complexity, vessel end points (number of vessels; Figure 3F), and vessel branchings (Figure 3G) were counted. *Mmp2* deficiency affected both parameters, but not the maximal distance separating the original limbus and the tips of neoformed lymphatics (Lmax; Figure 3H). These observations indicate increased complexity of the lymphatic vasculature in *Mmp2*-deficient mice (Figure 3B).

We next examined the neoformation of corneal lymphatic vessels by TEM (Figure 4A-F). The normal intact cornea is composed of lamellae of parallel collagenous bundles which cross at an angle to each other.[22] After cauterization, migrating LECs contained intracellular vesicles, extruded long processes probing the environment and progressively became aligned to form a cord (Figure 4A). In *Mmp2*-deficient mice, sections of neoformed lymphatics with parallel lumens were frequently seen (Figure 4B) and might reflect dichotomous branching of lymphatics. Collagen-fibril density also differed markedly between genotypes (Figure 4A-F). In WT mice, gaps were often seen between neighboring cells and extensive matrix remodeling and degradation were observed (Figure 4A,C,E). In sharp contrast, the meshwork of collagen fibrils remained much denser around LECs migrating in *Mmp2*-deficient mice (Figure 4B,D,F).

Lymphangioma formation was used as another in vivo model of MMP2-driven lymphangiogenesis (Figure 4G-J). In this system, LEC hyperplasia was induced by intraperitoneal incomplete Freund adjuvant injection leading to white lymphangioma masses appearing on the diaphragm surface. As previously described, lymphangioma development was reduced in *Mmp2* KO mice.[15] TEM analysis of lymphangioma largely confirmed the increased matrix remodeling seen in the cornea of WT mice (Figure 4E-F) where LECs were surrounded by processed matrix (Figure 4G), whereas intact collagen fibers were observed at the LEC-matrix interface in *Mmp2*-deficient mice (Figure 4H). Notably forking of lymphatic vessels was observed when migrating LECs abutted dense collagen matrix (Figure 4I-J).

Altogether these in vivo observations demonstrate that *Mmp2* deficiency in mice or down-regulation in zebrafish results in reduced vessel formation or altered vessel branching. They prompted us to postulate that lymphatic morphogenesis is driven by the physical constraints imposed by the ECM. Our working hypothesis is that LECs might adopt different phenotypes according to the extent of matrix remodeling: (1) A stationary phenotype in dense matrix. (2) A branching phenotype in case of local matrix deposition. (3) A mesenchymal-like migratory phenotype in case of controlled matrix degradation (Figure 5).

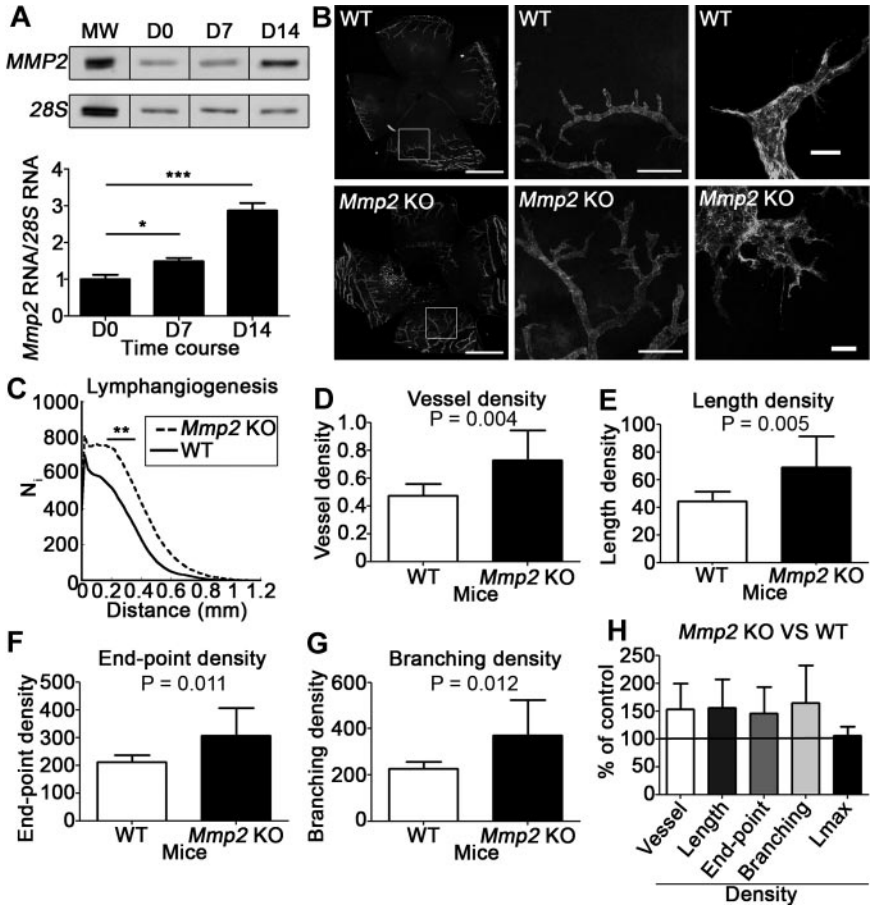

Figure 3. ***Mmp2*** **deficiency affects corneal lymphangiogenesis induced by thermal cauterization.** (A) RT-PCR analysis of *Mmp2* expression in the cornea in baseline (D0) and at 7 or 14 days after cornea cauterization. The graph depicts the densitometric quantification of *Mmp2* mRNA normalized to the *28S* signal. MW corresponds to molecular weight. (B) Lymphatic vessels were identified by LYVE-1 immunolabeling on whole-mount cornea issued from *Mmp2*-deficient mice (*Mmp2* KO) and WT mice. Left column: low-magnification images of the entire area (bars, 1 mm); middle column: higher magnification of the left-panel inserts (bars, 200 μm); Right column: highest magnification showing the tip of lymphatic buds (bars, 20 μm). (C-H) Computer-assisted quantification of lymphangiogenesis according to Blacher et al.[23] (C) Global analysis of lymphatic vessel distribution around the initial limbal vessel. (D-G) Additional parameters characterizing the vasculature were normalized to the total area of the cornea (density): area covered by neoformed vessels (vessel area density, D); total length of the vessels (vessel length density, E); number of vessels (end point density, F); number of bifurcations (branching density, G). (H) Results expressed as percentages of the control value reveal that *Mmp2* deficiency affected all parameters characterizing vasculature complexity, but not the maximal capillary length (Lmax). In panel B, left and middle columns, tissues stained with Alexa Fluor 488 (Molecular Probes) were used mounted in Vectashield mounting medium (Vector Laboratories), and images were captured at room temperature with AH3-RFCA fluorescent microscope (Olympus) coupled to DP72 digital camera (Olympus), using CellA 3.3 acquisition software (Olympus Soft Imaging Solutions) and a 4× NA 0.16 SPlan Apo lens (Olympus). Whole-mount pictures were assembled from 6 to 9 pictures with Photoshop CS4 software (Adobe Systems). In panel B, right column, tissues stained with Alexa Fluor 488 (Molecular Probes) were used mounted in Vectashield mounting medium (Vector Laboratories) and excited using a multi-Argon laser. Panels are Z-stack average projections of Z-series pictures that were acquired at room temperature, on a TCS SP2 confocal microscope (Leica Microsystems) with a 2 μm step size using Leica Confocal 2.5 acquisition software (Leica) and a 20× NA 0.4 N Plan L lens (Leica).

MMP2 drives in vitro LEC migration through collagen matrix

The direct contribution of MMP2 in LEC sprouting and migration into collagen matrix was evaluated by adding recombinant mouse MMP2 (rmMMP2) in the lymphatic ring assay. Lymphatic network development was stimulated when lymphatic rings embedded in a type I collagen gel were cultured with 50 ng/mL rmMMP2 ($P < .05$; Figure 6A). In this assay, the lymphangiogenic response was small when using TD rings derived from *Mmp2*-deficient mice (WT vs *Mmp2* KO: $P < .05$) and rescued by rmMMP2 administration (*Mmp2* KO vs *Mmp2* KO + rmMMP2: $P < .05$; Figure 6B).

To evaluate the role of the matrix composition and the physical resistance exerted by it against migrating cells, different matrices were used. (1) A reconstituted basement membrane (matrigel). (2) Pepsin-extracted type I collagen that does not contain the nonhelical telopeptides at the N and C-termini (pepsinized collagen). (3) Intact telopeptide-containing collagen (intact collagen). Because collagen telopeptides support the intermolecular covalent cross-links that stabilize gel architecture, their presence might affect LEC migration through the matrix as shown for tumor cells.[12] More LEC sprouting occurred in pepsinized collagen than native collagen (Figure 6C). In contrast, matrigel did not abet any LEC sprouting (data not shown). Intriguingly, the intact collagen concentration influenced LEC migration with a bell-shaped curve revealing optimal LEC migration at 2 mg/mL and impaired migration at lower (1.5 mg/mL) or higher (3 mg/mL) concentrations (Figure 6D). These findings clearly demonstrate the importance of LEC–matrix interactions in the lymphangiogenic process.

To further explore LECs migration within a 3-D matrix, we took advantage of a LEC spheroid assay that allows a time-lapse study to determine how cells move and interact with collagen fibers under confocal microscope. The suitability of this model was assessed by the impaired LEC migration observed through MMP2 inhibition with physiologic and synthetic inhibitors (supplemental Figure 1A-B, available on the *Blood* Web site; see the Supplemental Materials link at the top of the online article), as well as through siRNA-mediated MMP2 down-regulation (supplemental Figure

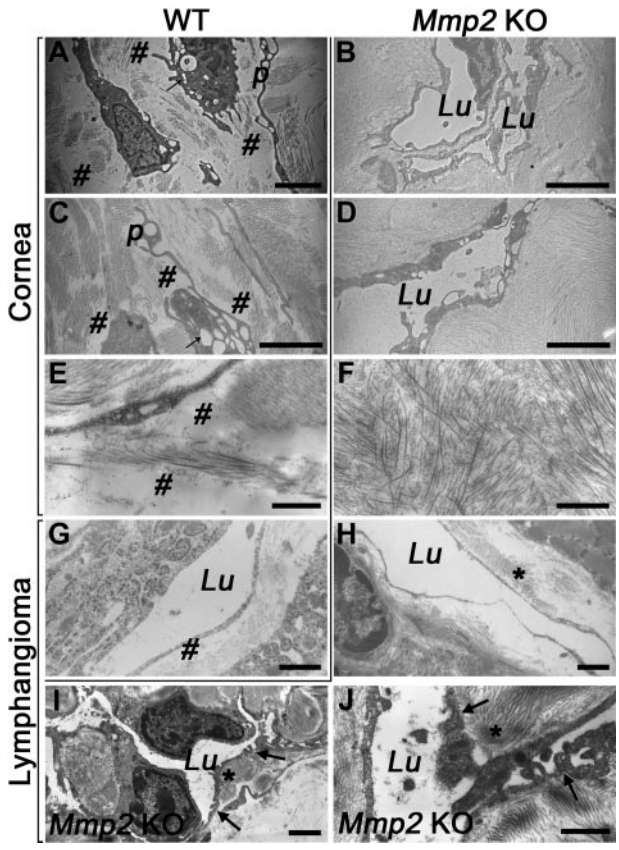

Figure 4. ***Mmp2*** **deficiency affects fibrillar collagen remodeling in vivo.** TEM of in vivo lymphangiogenesis induced by thermal cauterization of the cornea (A-F) and in lymphangioma (G-J), in WT (A,C,E,G) and *Mmp2* KO mice (B,D,F,H-J). (A-C) LECs form long processes (*p*) and contain intracellular vesicles (arrow). The ECM is extensively remodeled leading to numerous gaps between cells (#). (B-D) In the absence of *Mmp2*, LECs are surrounded by dense matrix and parallel lumens are often seen (B) in neoformed lymphatic vessels (*Lu*). (E-F) Higher magnification of the extensively remodeled collagen matrix (#) in WT mice (E), but reminiscent in KO mice (F). (G-H) Neoformed lymphatic vessels in lymphangioma surrounded by processed matrix (#) in WT mice (G), but dense matrix (*) in KO mice (H). (I-J) Lymphatic capillaries forking (arrows) around dense matrix (*) in *Mmp2*-deficient mice. Bars represent 5 μm (A-D), 1 μm (E,G,H) and 2 μm (F,I,J).

1C). Cell migration was partially rescued by adding rmMMP2 protein after siRNA treatment, further confirming the MMP2 implication in LEC migration. For real-time analysis of matrix degradation in live cells, collagen fibers were visualized by confocal reflection microscopy (Figure 7A-C). Under control conditions, migrating cells generated fiber traction and spatial reorganization (Figure 7A-B, supplemental Figure 2A-C). During the process of cell migration, collagen fiber degradation was visualized around cells leaving matrix gaps behind them (supplemental Figure 2A-C and supplemental Video 1). Fluorescent dequenching was assessed concomitantly with collagen-degradation visualization.[34,35] Therefore, DQ FITC–labeled collagen, which does not fluoresce until it is cleaved by a protease, was incorporated into the collagen gel containing multicellular LEC spheroids. Proteolysis was mainly visualized at the spheroid-matrix interface, and around isolated migrating cells (Figure 7D-E). The DQ signal of collagen degradation was not seen around filopodia-like extensions probing the environment, but mainly around the cell body (Figure 7D-F) and at the bases of the filopodial protrusion (Figure 7E; supplemental Video 2). The presence of intracellular and extracellular fluorescent collagen fragments was assessed on confocal microscopy after cell membrane labeling with a red cell membrane dye (supplemental Figure 2D). Pertinently, collagen-fiber reorganization (Figure 7G-I) and degradation (Figure 7J-L) were drastically reduced on exposure to MMP2 inhibition. In this setting, cells remained aggregated and extruded sensing cytoplasmic protrusions that continuously retracted and expanded (supplemental Video 3).

Discussion

How MMP2 regulates lymphangiogenesis is an intriguing question. We herein provide genetic and pharmacologic evidences that MMP2 activity contributes to lymphangiogenesis in pathologic conditions, during early lymphatic development, and in in vitro models of LEC sprouting from lymphatic duct rings or cell spheroids. Mechanistically, our study: (1) Underlines the importance of interstitial matrix remodeling during lymphangiogenesis. (2) Demonstrates that MMP2 acts in vivo as an interstitial collagenase, and not as a gelatinase as classically viewed. (3) Provides a model of mesenchymal cell migration and lymphatic vessel branching in a collagen-rich environment.

Our finding that *mmp2* knockdown in the zebrafish impairs, and even prevents lymphatic vessel formation in the most severely affected embryos is of great importance. So far, silencing of only a few genes (*Ccbe1, Vegfc, Vegfr3, syntenin, prox1, Notch/DLL4, claudin-like protein 24, lpa1*) has been shown to compromise zebrafish lymphatic development.[36] Our results provide the first evidence that an individual *mmp* knockdown drastically affects lymphatic vessel formation without modulating angiogenesis. In mice, *Mmp2* gene ablation led to transient changes in the complexity of early superficial dermal tail lymphatic formation, but did not affect later postnatal tail and ear adult lymphatic networks. The normal mature lymphatic vasculature observed in *Mmp2*-deficient mice could reflect compensation by other MMPs exerting similar functions, supporting the overall complexity of the murine system.[37] In sharp contrast, under challenging conditions, *Mmp2* down-regulation or knockdown resulted in lymphatic vasculature abnormalities characterized by reduced vessel formation (spheroid and lymphatic ring assays) or increased vessel branchings (mouse

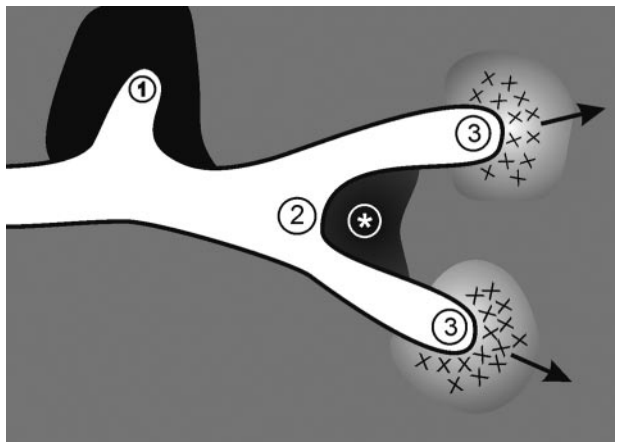

Figure 5. **Proposed morphogenic mechanism mediated by MMP2.** Our working hypothesis is that LEC behavior is driven by physical constraints imposed by the matrix barrier. Lymphatic vessel elongation and/or branching are dictated by the composition of ECM components, the quantity and cross-linking of the components and where they are situated around the developing vessels. The structural and molecular determinants promote: (1) a stationary phenotype in dense matrix; (2) a bifurcation in case of local matrix deposition as delineated by * (see also Figure 4I-J); and (3) a mesenchymal-like migratory phenotype in case of controlled matrix degradation.

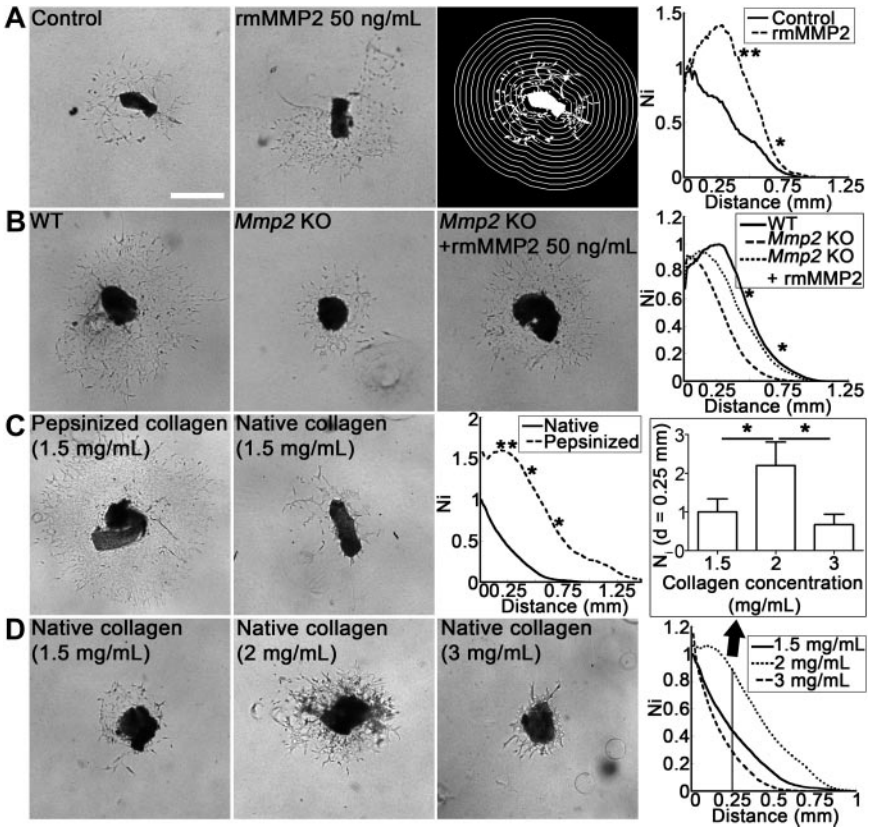

Figure 6. MMP2 and type-1 collagen matrix influence in vitro lymphangiogenesis in the lymphatic ring assay. (A) Mouse lymphatic duct explants embedded in type I collagen gel were cultured for 9 days in the absence (control) or presence of recombinant MMP2 (rmMMP2 50 ng/mL). For quantification, grid corresponding to successive increments at fixed intervals of TD boundary was used on binarized images (right panel). The number of microvessel–grid intersections (N_i) was quantified on binarized images as described in "Lymphatic ring assay." (B) Lymphatic rings issued from *Mmp2*-deficient mice were cultured without (*Mmp2* KO) or with rmMMP2 (*Mmp2* KO + rmMMP2). Rings issued from WT mice were used as control (WT). (C) Lymphatic duct explants were embedded in pepsinized or native collagen gel (final concentration, 1.5 mg/mL). (D) Native collagen gels contained 1.5, 2, or 3 mg/mL, revealing optimal migration at 2 mg/mL and less migration at higher and lower concentrations. Graphs represent computerized quantifications of LECs distribution around the ring at day 9. The histogram corresponds to LECs density at a distance (d) = 0.25 mm from the ring border. N_i = Number of intersections between microvessels and quantification grid. Values were normalized by taking the maximum of the control curve as 1. For all assays, the images presented are a representative 1 of all rings used for quantification ($n \geq 5$; $^*P < .05$; $^{**}P < .001$). Bars represent 500 μm. Unstained live tissues were used in their culture medium, and images were captured with a phase-contrast microscope (Axiovert 25; Carl Zeiss Microscopy) coupled to an Axiocam color digital camera (Carl Zeiss), at room temperature using acquisition software KS400 3.0 (Carl Zeiss Vision) and a 5× NA 0.12 A-Plan lens (Carl Zeiss).

cornea or dermal tail). These apparently contrasting findings led us to postulate that MMP2 is a key morphogenic regulator of lymphatic vessels. By analogy to branching morphogenesis occurring in epithelial structures, such as mammary, lung, kidney, and salivary glands,[38-40] we hypothesize that an adequate balance between proteases and protease inhibitors orchestrates cell migration through the meshwork of the ECM. An adequate density of appropriately cross-linked collagen fibers is required for vessel formation as both excessive or insufficient matrix impairs LEC sprouting. Such requirement of finely balanced matrix degradation has been reported during angiogenesis and involves at least, the plasminogen/plasmin proteolytic system controlled by plasminogen activator inhibitor-1.[41,42] We thus postulated that inhibition or absence of MMP2 activity leads either to impaired lymphatic vessel extension through limited degradation of physically constraining ECM, or increased vessel bifurcation through increased focal matrix deposition.

This concept of branching morphogenesis implies that vessel elongation and branching are dictated by the ECM component composition, amount, and cross-link status. This is indeed supported by TEM observations in in vivo models (corneal lymphangiogenesis assay and lymphangioma), revealing that lymphatic vessel branched when facing a dense collagen barrier. Furthermore, LEC migration in vitro was influenced by collagen concentration and intermolecular covalent cross-links that stabilize collagen-gel architecture.[12] MMP2-selective inhibition or *MMP2*-silencing inhibited LEC migration in a collagen scaffold. This inhibitory effect was associated with less collagen-fiber degradation as assessed by dynamic imaging and detection of the DQ FITC–labeled collagen fibers. Accordingly, TEM analysis revealed that lymphatic vessels formed through tunneling, relying on extensive matrix remodeling, migration and alignment of sprouting endothelial cells into tubular structures.[22] In line with this tunneling concept, intracellular fragments of collagen have been visualized by confocal microscopy. Altogether, these observations indicate that LECs adopt a proteolysis-driven mesenchymal migration program primarily dependent on MMP2. Time-lapse video-microscopy applied to the spheroid model shows that the spatial organization of pericellular collagen fibers is modified during the process of LEC migration. Collagen-fiber cleavage occurred mainly around cell bodies instead of cell protrusions suggesting that filopodia-like extensions sense their environment but do not drive the proteolysis-dependent migration. This notion agrees with previous observations made with tumor cells.[34] Herein, we demonstrated that LECs use MMP2 to remodel the collagen meshwork to ease their passage through a physical barrier. Optimal migration was only achieved when LECs were in contact with an appropriate collagen matrix. Such a specific

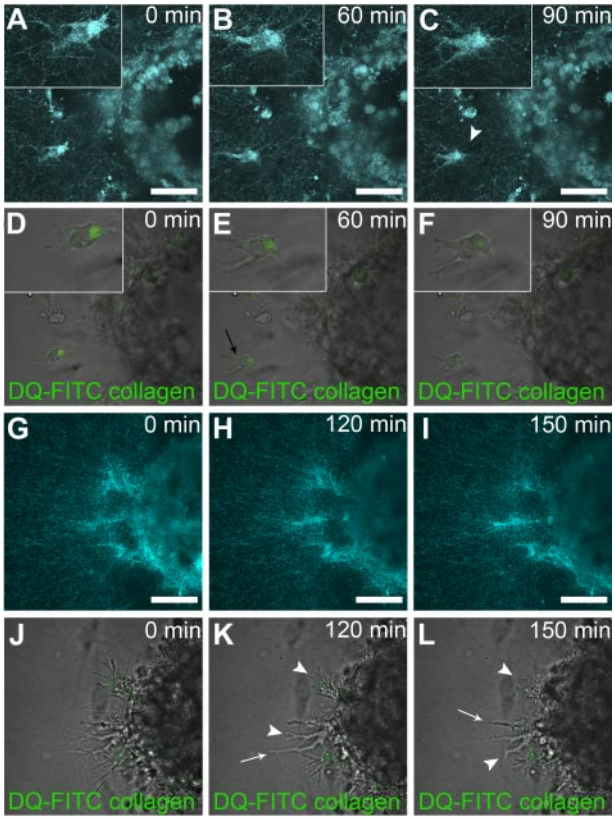

Figure 7. Proteolytic-driven migration of HTERT-HDLECs cells into 3-D collagen gels. Spheroid and collagen fibers are visualized with a reflectance process (A-C,G-I). Dequenched (DQ) FITC collagen (green) becoming fluorescent after cleavage is used to visualize matrix degradation (D-F,J-L). (A-F) Insets show higher magnification of migrating cells. Under control conditions (A-F), a sprouting cell extends protrusion sensing the environment (A-B). Collagen degradation leads to a hole behind moving cell (C; see also supplemental Figure 2). Cleaved collagen appears in the cells (D-F) and at pseudopod–cell body interface (arrow; E). After MMP2 inhibition (G-L), no cell detached from the spheroid (G-I) and cleaved collagen is absent after MMP2 inhibition (J-L). On inhibitor treatment, cells extrude (white arrow) and retract (arrow head) pseudopods (K-L). Bars represent 50 μm in each panel. Live tissues were used in their culture medium and time-lapse imaging was performed using a Fluoview FV1000 confocal microscope (Olympus) at 37°C with Fluoview 3.0a acquisition software (Olympus) and a 60× NA 1.35 UPL SAPO lens (Olympus).

interaction between LECs and interstitial matrix is further supported by the failure of LECs to sprout of a lymphatic duct ring embedded in basement membrane matrix (matrigel).

It is worth noting that MMP2 could affect lymphatic vessel morphogenesis at levels beyond the impact of the physical barrier. By degrading the collagen scaffolds, MMP2 might also promote the release of ECM-sequestered lymphangiogenic regulators. In this context, MMP2-triggered FGF-2 release from the lens capsule is essential for lens epithelial cell survival.[43] In addition, signaling through cell-matrix receptors could be modified in less remodeled matrix.[44] Alternatively, neo-epitopes, cryptic in intact collagen fibrils, might be exposed after MMP2 cleavage, thereby providing new morphogenetic signals.[45] These different mechanisms are obviously not exclusive.

When matrix remodeling is considered, MMP2 is primarily viewed as a type IV collagenase and a gelatinase contributing to the degradation of collagen fragments generated by the so-called interstitial collagenases. Our findings clearly underline the interstitial collagenolytic activity of MMP2. Although the capacity of MMP2 to cleave fibrillar type I collagen was described > 15 years ago,[46,47] such collagenolytic activity has been overshadowed and deserves more attention than initially expected. Using an siRNA approach, we modulated the expressions of secreted MMP (MMP2) and membrane-type MMP (MT1-MMP) produced by LECs, and known to cleave type I collagen.[48] Although *MMP2* knockdown impaired LEC migration in a 3-D collagen matrix, *MT1-MMP* down-regulation had no impact (data not shown). This observation underscores the unexpected role of MMP2, but not that of MT1-MMP, in the collagenolytic pathway implicated in lymphangiogenesis. It implies to revisit the role of MMP2 in cell migration.

Notably, the present study demonstrates that interstitial collagen remodeling is a rate-limiting event in lymphangiogenesis. This observation agrees with the Podgrabinska et al report,[49] which shows that in the absence of exogenous factors, LECs incorporated into collagen type I scaffolds exhibited a significantly higher survival rate than blood endothelial cells (BECs). This difference between LEC and BEC responses to type I collagen probably mirrors matrix differences surrounding each endothelial cell type in its natural environment (interstitial matrix and basement membrane, respectively). LEC migration requires cells to deal with a connective tissue dominated by a cross-linked type I collagen network. MMP2, an established regulator of tumor invasion and angiogenesis, acts mainly through its gelatinolytic activity and capacity to regulate growth factor bioavailability/activity. Herein, we provide new mechanistic insights into its crucial role during lymphangiogenesis and shed light on MMP2 collagenolytic function. Experiments addressing how LECs interact with their surrounding ECM environment will undoubtedly enhance our understanding of lymphatic vessel formation and functional regulation under physiologic and pathologic conditions.

Acknowledgments

The authors acknowledge the contribution of researchers from the GIGA (Zebrafish Platform, Animal Facility Platform, Imaging and Flow Cytometry Platform) and G. Roland, M. Dehuy, N. Decloux, I. Dasoul, E. Feyereisen, L. Poma, P. Gavitelli, and L. Volders. They thank Professor Schulte-Merker for providing the Stab1:YFP zebrafish line and Professor M. Pepper for providing the HTERT-HDLEC cells.

This work was supported by grants from the European Union Framework Program projects (FP7-2007-2011 "MICROENVIMET" no. 201279), the Fonds de la Recherche Scientifique Médicale, the Fonds National de la Recherche Scientifique (FNRS, Belgium), the Fondation contre le Cancer, the Fonds spéciaux de la Recherche (University of Liège), the "Plan Cancer" (Belgium), the Center Anticancéreux près l'Université de Liège, the Fonds Léon Fredericq (University of Liège), the Direction Générale des Technologies, de la Recherche et de l'Energie from the Région Wallonne, and the Interuniversity Attraction Poles Program–Belgian Science Policy. B.D., C.E., and C.B. each received a Televie-FNRS grant.

Authorship

Contribution: B.D., C.E., J.P., T.R., and C.M. performed experiments, analyzed data, and made the figures; S.B. developed data analysis tools; F.B., M.T., H.P., V.L., C.B., S.O., and F.L. contributed to data analysis; L.M. and E.J. contributed to zebrafish experiments; L.M., D.C., F.K., P.C., J.-M.F., and I.S. contributed to data interpretation and made critical review of the paper; and

A.N. interpreted data, designed and coordinated the study, and wrote the paper.

Conflict-of-interest disclosure: The authors declare no competing financial interests.

Correspondence: Agnès Noël, Laboratory of Tumor and Developmental Biology, University of Liège, Tour de Pathologie, CHU (B23), Sart Tilman, B-4000 Liège, Belgium; e-mail: agnes.noel@ulg.ac.be.

References

1. Ellenberg D, Azar DT, Hallak JA, et al. Novel aspects of corneal angiogenic and lymphangiogenic privilege. *Prog Retin Eye Res.* 2010;29(3):208-248.
2. Karpanen T, Alitalo K. Molecular biology and pathology of lymphangiogenesis. *Annu Rev Pathol.* 2008;3:367-397.
3. Sleeman JP, Thiele W. Tumor metastasis and the lymphatic vasculature. *Int J Cancer.* 2009; 125(12):2747-2756.
4. Achen MG, Stacker SA. Molecular control of lymphatic metastasis. *Ann N Y Acad Sci.* 2008;1131: 225-234.
5. Avraamides CJ, Garmy-Susini B, Varner JA. Integrins in angiogenesis and lymphangiogenesis. *Nat Rev Cancer.* 2008;8(8):604-617.
6. Tammela T, Alitalo K. Lymphangiogenesis: Molecular mechanisms and future promise. *Cell.* 2010;140(4):460-476.
7. Williams SP, Karnezis T, Achen MG, Stacker SA. Targeting lymphatic vessel functions through tyrosine kinases. *J Angiogenes Res.* 2010;2:13.
8. Bignon M, Pichol-Thievend C, Hardouin J, et al. Lysyl oxidase-like protein-2 regulates sprouting angiogenesis and type IV collagen assembly in the endothelial basement membrane. *Blood.* 2011;118(14):3979-3989.
9. Paupert J, Sounni NE, Noel A. Lymphangiogenesis in post-natal tissue remodeling: lymphatic endothelial cell connection with its environment. *Mol Aspects Med.* 2011;32(2):146-158.
10. Wiig H, Keskin D, Kalluri R. Interaction between the extracellular matrix and lymphatics: consequences for lymphangiogenesis and lymphatic function. *Matrix Biol.* 2010;29(8):645-656.
11. Garmy-Susini B, Avraamides CJ, Schmid MC, et al. Integrin alpha4beta1 signaling is required for lymphangiogenesis and tumor metastasis. *Cancer Res.* 2010;70(8):3042-3051.
12. Sabeh F, Shimizu-Hirota R, Weiss SJ. Protease-dependent versus -independent cancer cell invasion programs: three-dimensional amoeboid movement revisited. *J Cell Biol.* 2009;185(1): 11-19.
13. Wolf K, Mazo I, Leung H, et al. Compensation mechanism in tumor cell migration: mesenchymal-amoeboid transition after blocking of pericellular proteolysis. *J Cell Biol.* 2003;160(2):267-277.
14. Kessenbrock K, Plaks V, Werb Z. Matrix metalloproteinases: regulators of the tumor microenvironment. *Cell.* 2010;141(1):52-67.
15. Bruyere F, Melen-Lamalle L, Blacher S, et al. Modeling lymphangiogenesis in a three-dimensional culture system. *Nat Methods.* 2008; 5(5):431-437.
16. Nakamura ES, Koizumi K, Kobayashi M, Saiki I. Inhibition of lymphangiogenesis-related properties of murine lymphatic endothelial cells and lymph node metastasis of lung cancer by the matrix metalloproteinase inhibitor MMI270. *Cancer Sci.* 2004;95(1):25-31.
17. Dean RA, Butler GS, Hamma-Kourbali Y, et al. Identification of candidate angiogenic inhibitors processed by matrix metalloproteinase 2 (MMP-2) in cell-based proteomic screens: disruption of vascular endothelial growth factor (VEGF)/heparin affin regulatory peptide (pleiotrophin) and VEGF/Connective tissue growth factor angiogenic inhibitory complexes by MMP-2 proteolysis. *Mol Cell Biol.* 2007;27(24):8454-8465.
18. Bauvois B. New facets of matrix metalloproteinases MMP-2 and MMP-9 as cell surface transducers: Outside-in signaling and relationship to tumor progression. *Biochim Biophys Acta.* 2012; 1825(1):29-36.
19. Cauwe B, Van den Steen PE, Opdenakker G. The biochemical, biological, and pathological kaleidoscope of cell surface substrates processed by matrix metalloproteinases. *Crit Rev Biochem Mol Biol.* 2007;42(3):113-185.
20. Thisse C, Thisse B, Schilling TF, Postlethwait JH. Structure of the zebrafish snail1 gene and its expression in wild-type, spadetail and no tail mutant embryos. *Development.* 1993;119(4):1203-1215.
21. Masson V, de la Ballina LR, Munaut C, et al. Contribution of host MMP-2 and MMP-9 to promote tumor vascularization and invasion of malignant keratinocytes. *FASEB J.* 2005;19(2):234-236.
22. Detry B, Bruyere F, Erpicum C, et al. Digging deeper into lymphatic vessel formation in vitro and in vivo. *BMC Cell Biol.* 2011;12(1):29.
23. Blacher S, Detry B, Bruyere F, Foidart JM, Noel A. Additional parameters for the morphometry of angiogenesis and lymphangiogenesis in corneal flat mounts. *Exp Eye Res.* 2009;89(2):274-276.
24. Tripp CH, Haid B, Flacher V, et al. The lymph vessel network in mouse skin visualised with antibodies against the hyaluronan receptor LYVE-1. *Immunobiology.* 2008;213(9-10):715-728.
25. Nisato RE, Harrison JA, Buser R, et al. Generation and characterization of telomerase-transfected human lymphatic endothelial cells with an extended life span. *Am J Pathol.* 2004; 165(1):11-24.
26. Sounni NE, Rozanov DV, Remacle AG, Golubkov VS, Noel A, Strongin AY. Timp-2 binding with cellular MT1-MMP stimulates invasion-promoting MEK/ERK signaling in cancer cells. *Int J Cancer.* 2010;126(5):1067-1078.
27. Fusenig NE, Limat A, Stark HJ, Breitkreutz D. Modulation of the differentiated phenotype of keratinocytes of the hair follicle and from epidermis. *J Dermatol Sci.*1994;7(suppl):S142-S151.
28. Hammer T, Tritsaris K, Hubschmann MV, et al. IL-20 activates human lymphatic endothelial cells causing cell signalling and tube formation. *Microvasc Res.* 2009;78(1):25-32.
29. Bruyere F, Melen-Lamalle L, Blacher S, et al. Does plasminogen activator inhibitor-1 drive lymphangiogenesis? *PloS one.* 2010;5(3):e9653.
30. Mancardi S, Stanta G, Dusetti N, et al. Lymphatic endothelial tumors induced by intraperitoneal injection of incomplete Freund's adjuvant. *Exp Cell Res.* 1999;246(2):368-375.
31. Xu Y, Yuan L, Mak J, et al. Neuropilin-2 mediates VEGF-C-induced lymphatic sprouting together with VEGFR3. *J Cell Biol.* 2010;188(1):115-130.
32. Zhang J, Bai S, Zhang X, Nagase H, Sarras MP, Jr. The expression of gelatinase A (MMP-2) is required for normal development of zebrafish embryos. *Dev Genes Evol.* 2003;213(9):456-463.
33. Yaniv K, Isogai S, Castranova D, Dye L, Hitomi J, Weinstein BM. Live imaging of lymphatic development in the zebrafish. *Nat Med.* 2006;12(6): 711-716.
34. Friedl P, Wolf K. Proteolytic interstitial cell migration: a five-step process. *Cancer Metastasis Rev.* 2009;28(1-2):129-135.
35. Sameni M, Cavallo-Medved D, Dosescu J, et al. Imaging and quantifying the dynamics of tumor-associated proteolysis. *Clin Exp Metastasis.* 2009;26(4):299-309.
36. Schulte-Merker S, Sabine A, Petrova TV. Lymphatic vascular morphogenesis in development, physiology, and disease. *J Cell Biol.* 2011;193(4): 607-618.
37. Puente XS, Sanchez LM, Overall CM, Lopez-Otin C. Human and mouse proteases: a comparative genomic approach. *Nat Rev Genet.* 2003;4(7): 544-558.
38. Fata JE, Werb Z, Bissell MJ. Regulation of mammary gland branching morphogenesis by the extracellular matrix and its remodeling enzymes. *Breast Cancer Res.* 2004;6(1):1-11.
39. Kheradmand F, Rishi K, Werb Z. Signaling through the EGF receptor controls lung morphogenesis in part by regulating MT1-MMP-mediated activation of gelatinase A/MMP2. *J Cell Sci.* 2002; 115(Pt 4):839-848.
40. Wiseman BS, Sternlicht MD, Lund LR, et al. Site-specific inductive and inhibitory activities of MMP-2 and MMP-3 orchestrate mammary gland branching morphogenesis. *J Cell Biol.* 2003; 162(6):1123-1133.
41. Lambert V, Munaut C, Carmeliet P, et al. Dose-dependent modulation of choroidal neovascularization by plasminogen activator inhibitor type I: implications for clinical trials. I*nvest Ophthalmol Vis Sci.* 2003;44(6):2791-2797.
42. Devy L, Blacher S, Grignet-Debrus C, et al. The pro- or antiangiogenic effect of plasminogen activator inhibitor 1 is dose dependent. *FASEB J.* 2002;16(2):147-154.
43. Tholozan FM, Gribbon C, Li Z, et al. FGF-2 release from the lens capsule by MMP-2 maintains lens epithelial cell viability. *Mol Biol Cell.* 2007; 18(11):4222-4231.
44. Rupp PA, Visconti RP, Czirok A, Cheresh DA, Little CD. Matrix metalloproteinase 2-integrin alpha(v)beta3 binding is required for mesenchymal cell invasive activity but not epithelial locomotion: a computational time-lapse study. *Mol Biol Cell.* 2008;19(12):5529-5540.
45. Deryugina EI, Quigley JP. Pleiotropic roles of matrix metalloproteinases in tumor angiogenesis: contrasting, overlapping and compensatory functions. *Biochim Biophys Acta.* 2010;1803(1):103-120.
46. Aimes RT, Quigley JP. Matrix metalloproteinase-2 is an interstitial collagenase. Inhibitor-free enzyme catalyzes the cleavage of collagen fibrils and soluble native type I collagen generating the specific 3/4- and 1/4-length fragments. *J Biol Chem.* 1995;270(11):5872-5876.
47. Egeblad M, Shen HC, Behonick DJ, et al. Type I collagen is a genetic modifier of matrix metalloproteinase 2 in murine skeletal development. *Dev Dyn.* 2007;236(6):1683-1693.
48. Maquoi E, Assent D, Detilleux J, Pequeux C, Foidart JM, Noel A. MT1-MMP protects breast carcinoma cells against type I collagen-induced apoptosis. *Oncogene.* 2012;31(4):480-493.
49. Podgrabinska S, Braun P, Velasco P, Kloos B, Pepper MS, Skobe M. Molecular characterization of lymphatic endothelial cells. *Proc Natl Acad Sci U S A.* 2002;99(25):16069-16074.